ISSN 1063-7826, Semiconductors, 2015, Vol. 49, No. 3, pp. 394–400. © Pleiades Publishing, Ltd., 2015.
Original Russian Text © G.S. Khrypunov, O.V. Pirohov, T.A. Gorstka, V.A. Novikov, N.A. Kovtun, 2015, published in Fizika i Tekhnika Poluprovodnikov, 2015, Vol. 49, No. 3, pp. 406–412.

PHYSICS OF SEMICONDUCTOR DEVICES

Effect of Nanoscale Tin-Dioxide Layers on the Efficiency of CdS/CdTe-Based Film Solar Elements

G. S. Khrypunov^, O. V. Pirohov, T. A. Gorstka, V. A. Novikov, and N. A. Kovtun

Kharkiv Polytechnic Institute, Kharkiv, 61002 Ukraine

Shevchenko State University, Kyiv, 03680 Ukraine

^e-mail: khrip@ukr.net

Submitted April 8, 2014; accepted for publication June 16, 2014

Abstract—Comparative investigations of the output parameters and optical diode characteristics of ITO/CdS/CdTe/Cu/Au and SnO_2 : F/CdS/CdTe/Cu/Au film solar cells are carried out with the aim of optimizing the design of the front electrodes. It is established that the high voltage and large filling factor of the solar elements with SnO_2 : F films are caused by a lower diode saturation current density and series resistance due to the stability of the crystal structure and electrical properties of these films against chloride treatment of the base layer during device fabrication. At the same time, solar elements with an ITO front electrode exhibit a higher short-circuit current density due to the larger average light transmittance of the ITO layers. The use of nanoscale SnO_2 layers in the ITO front contacts allows the efficiency of the CdS/CdTe-based solar elements to be enhanced to 11.4% on account of stabilization of the crystal structure and electrical properties of the ITO films and a possible reduction in the cadmium-sulphide-layer thickness without shunting the device structure.

DOI: 10.1134/S1063782615030112

1. INTRODUCTION

Cadmium-telluride films exhibit high absorbance and have a band gap optimal for the photoelectric transformation of solar radiation under terrestrial conditions, which make these materials promising candidates for application as the base layers of high-efficiency and low-cost solar cells (SCs) [1]. Modern film SCs based on cadmium sulphide and telluride are fabricated in the superstrate configuration [2]. In such a construction, the device structure is formed on a glass substrate through which solar radiation enters the base layer. In such SCs, first a front transparent electrode film is formed and then high-temperature technological operations of the CdS/CdTe heterosystem formation are performed, during the course of which the initial optical and electrical properties of the front electrodes can be changed. Enhancement of the front-electrode surface resistance reduces SC efficiency due to an increase in the series resistance of the entire device structure. A reduction in the transmittance of the front electrode reduces the SC efficiency because of a decrease in the density of the photon flux entering the base layer.

In the superstrate CdS/CdTe-based SC front electrodes, ITO (indium tin oxide) and SnO_2 : F layers are traditionally used [3]. Therefore, to optimize the design of the CdS/CdTe-based film SC front electrodes, we carry out comparative investigations of devices with indium and tin oxide-based front electrodes.

2. EXPERIMENTAL

The CdS/CdTe-based film SCs were formed on glass substrates with ITO and SnO_2 : F front electrodes (Nippon Sheet Company). The ITO and SnO_2 : F film thicknesses (d) were 120 and 380 nm, respectively. In some of the SCs, thin undoped tin-oxide films were deposited onto the ITO layers by nonreactive dc magnetron sputtering using a VUP-5M vacuum facility at a substrate temperature of 300°C. On the surface of the three types of front electrodes (ITO, SnO_2 : F, and ITO/SnO_2), cadmium-sulphide films with a thickness of $d_{CdS} = (0.2–0.4)$ μm were deposited by thermal vacuum evaporation at a substrate temperature of 200°C via a modernized UVN vacuum facility; then, without loss of vacuum, 4-μm-thick cadmium-telluride layers were formed. The obtained heterosystems were subjected to chloride treatment, which represents a standard technological operation of the fabrication of high-efficiency CdS/CdTe-based SEs [2]. For this purpose, $CdCl_2$ layers were deposited onto the CdTe surface without heating of the substrate and annealed in air at a temperature of 430°C for 25 min. After annealing, the base layer was etched in a bromine-methanol solution to eliminate products of the chemical reaction occurring during chloride treatment and obtain a nanoscale tellurium spacer layer on the CdTe surface for the formation of a high-efficiency tunnel contact. After etching by the method of thermal vacuum evaporation, Cu/Au films with respective thick-

Table 1. Output parameters and "light" diode characteristics of ITO/CdS/CdTe/Cu/Au and SnO_2 : F/CdS/CdTe/Cu/Au solar cells treated by means of cadmium-chloride layers of different thicknesses

Output parameters and "light" diode characteristics	ITO			SnO_2 : F		
	$d_{CdCl_2} = 0.2$ μm	$d_{CdCl_2} = 0.4$ μm	$d_{CdCl_2} = 0.6$ μm	$d_{CdCl_2} = 0.4$ μm	$d_{CdCl_2} = 0.6$ μm	$d_{CdCl_2} = 0.8$ μm
J, mA/cm^2	19.8	21.1	19.7	16.9	19.6	19.2
U, mV	640	734	643	758	778	719
FF, rel. units	0.58	0.62	0.64	0.56	0.64	0.67
η, %	7.4	9.5	8.1	7.2	9.8	9.3
J_{ph}, mA/cm^2	19.9	21.1	19.8	17.5	19.8	19.5
R_p, Ω cm^2	2.8	5.0	3.0	7.2	4.0	3.8
R_{sh}, Ω cm^2	855	580	624	405	680	556
A, rel. units	2.8	2.5	2.6	2.3	2.0	2.7
J_0, A/cm^2	4.4×10^{-7}	6.3×10^{-8}	5.3×10^{-7}	5.7×10^{-8}	2.5×10^{-8}	4.1×10^{-8}

nesses of 11 and 50 nm were deposited and annealed in vacuum at a temperature of 200°C for 20 min.

To determine the output parameters, including the short-circuit current density J, open-circuit voltage U, filling factor FF of the "light" I–V characteristic, and efficiency η under irradiation with an optical beam with a power of 100 mW/cm^2, we measured the "light" I–V characteristics. Using an LED display, we obtained an optical beam with a spectral composition corresponding to the solar-radiation spectrum under terrestrial conditions.

According to the equivalent circuit [4], the quantitative characteristics of the photoelectric processes occurring under SC illumination are "light" diode characteristics, including the photocurrent density J_{ph}, diode saturation current density J_0, diode perfection factor A, and the series and shunting resistances R_p and R_{sh} per unit of active area of the device structure. The correlation of the SC efficiency and the "light" diode characteristics is implicitly described by the theoretical I–V characteristic of a SC [4]

$$J_{ch} = -J_{ph} + J_0\{\exp[e(U_{ch} - J_{ch}R_p)/(AkT)] - 1\} + (U_{ch} - JR_p)/R_{sh}, \quad (1)$$

where J_{ch} is the density of current flowing through the load, e is the elementary charge, k is the Boltzmann constant, T is the solar-cell temperature, and U_{ch} is the voltage drop at the load.

The output parameters and the "light" diode characteristics of the SCs were determined by approximation of the experimental "light" I–V characteristics using theoretical expression (1). Upon analytical processing, the root-mean-square deviation of the theoretical I–V characteristic from the experimental one was no larger than 10^{-8}, which corresponds to a relative error in determination of the output parameters and "light" diode characteristics of no more than 1%.

3. EXPERIMENTAL RESULTS

3.1. Effect of the ITO and SnO_2 : F Front Electrodes on the Efficiency of CdS/CdTe-Based Solar Cells

We measured the "light" I–V characteristics of ITO/CdS/CdTe/Cu/Au SC laboratory samples which had undergone treatment via the application of cadmium-chloride layers of different thicknesses d_{CdCl_2}. Through analytical processing of the "light" I–V characteristics, we determined the output parameters and "light" diode characteristics of the fabricated SCs. We separated a few typical ranges of the cadmium-chloride layer thickness, which correspond to a change in the physical mechanisms of the d_{CdCl_2} effect on η. The efficiency, output parameters, and "light" diode characteristics corresponding to these ranges are given in Table 1. It can be seen that d_{CdCl_2} growth to 0.4 μm leads to an increase in η to 9.5% as a result of an increase in U, J, and FF. With a further increase in d_{CdCl_2} to 0.6 μm, the efficiency decreases to 8.1% due to a decrease in U and J.

To analyze the quantitative effect of the "light" diode characteristics on the experimentally observed efficiency variation, we mathematically simulated the effect of the "light" diode characteristics on the theoretical "light" I–V characteristic. In the simulation, we used the "light" diode characteristics of SCs with η = 7.4 and 9.5% (Table 1). For each SC at a fixed set of four "light" diode characteristics obtained by analytical processing of the experimental "light" I–V characteristics, the effect of the variation in the remaining diode characteristic on the efficiency in the experimentally determined range of values was simulated. For this purpose, we substituted the values for five "light" diode characteristics in theoretical expression (1), constructed the theoretical "light" I–V characteristic, and determined the theoretical SC effi-

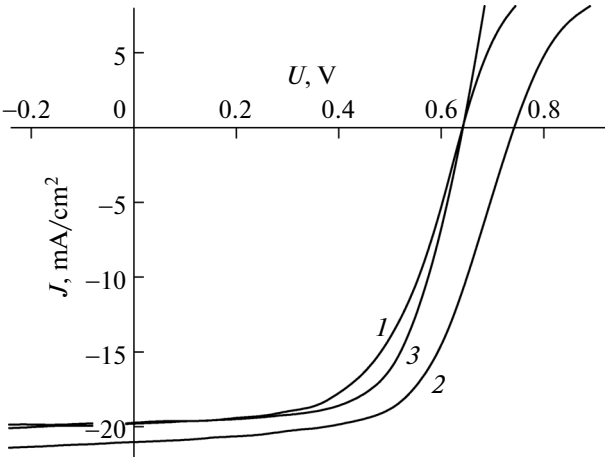

Fig. 1. "Light" I–V characteristics of the ITO/CdS/CdTe/Cu/Au solar cells. d_{CdCl_2} = (*1*) 0.2, (*2*) 0.4, and (*3*) 0.6 μm.

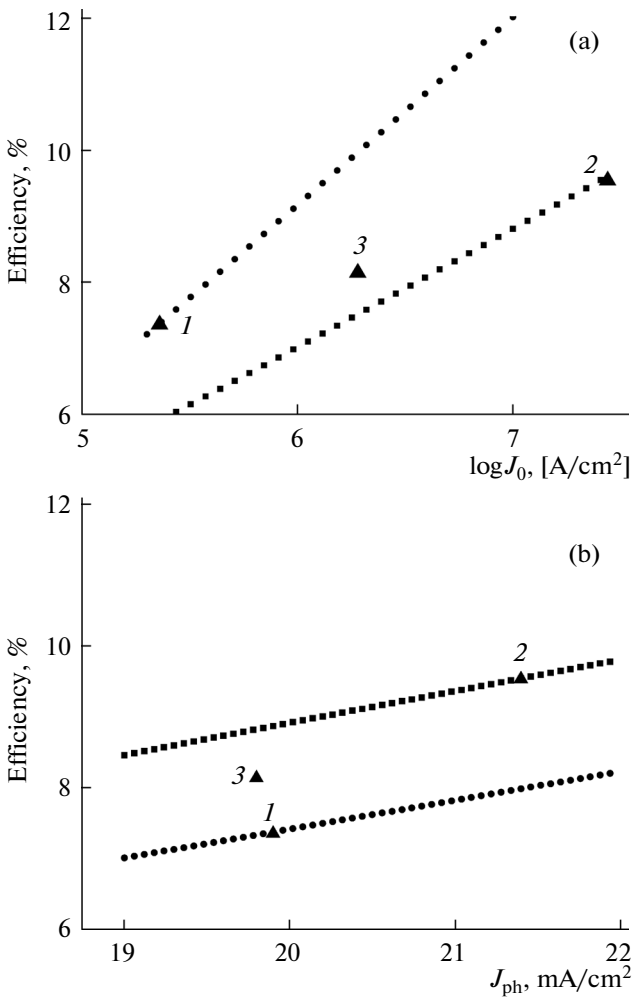

Fig. 2. Simulation of the effect of the "light" diode characteristics on the efficiency of the ITO/CdS/CdTe/Cu/Au solar cells. d_{CdCl_2} = (*1*) 0.2, (*2*) 0.4, and (*3*) 0.6 μm.

ciency. Then, the procedure was repeated many times for other sets of "light" diode characteristics. As a result, we obtained the theoretical dependence of the SC efficiency on the variation in one diode characteristic in the chosen range of values with the remaining four characteristics being fixed (see, for example, Fig. 2). In the plot graphs, the experimental η values were also marked. It was established that the growth in the efficiency of the ITO/CdS/CdTe/Cu/Au SC from η = 7.4% to η = 9.5% with an increase in the cadmium-chloride thickness from d_{CdCl_2} = 0.2 μm to d_{CdCl_2} = 0.4 μm is due to a decrease in the diode saturation current density from $J_0 = 4.4 \times 10^{-7}$ A/cm^2 to $J_0 = 6.3 \times 10^{-8}$ A/cm^2 (Table 1 and Fig. 2a). Variation in the other diode characteristics does not significantly affect the experimentally observed efficiency variation (Fig. 2b). A reduction in the diode saturation current density indicates enhancement of the separating barrier quality and growth in the lifetime of nonequilibrium carriers generated by light. It was demonstrated that the experimentally observed efficiency drop from η = 9.5% to η = 8.1% with a further increase in the cadmium-chloride thickness from d_{CdCl_2} = 0.4 μm to d_{CdCl_2} = 0.6 μm can be simulated by growth in the diode saturation current density from $J_0 = 6.3 \times 10^{-8}$ A/cm^2 to $J_0 = 5.3 \times 10^{-7}$ A/cm^2 (Table 1 and Fig. 2b).

We investigated the effect of the cadmium-chloride-layer thickness during "chloride" treatment on the output parameters and "light" diode characteristics of the SnO_2 : F/CdS/CdTe/Cu/Au SCs. Analytical processing of the "light" I–V characteristics of the SnO_2 : F/CdS/CdTe/Cu/Au SCs (Fig. 1b) shows that at a $CdCl_2$-layer thickness of 0.6 μm, the maximum efficiency (9.7%) is observed. It can be seen from Table 1 that the growth of η to 9.7% with an increase in the cadmium-chloride-layer thickness to d_{CdCl_2} = 0.6 μm results from an increase in all output parameters. With a further increase in the thickness, η decreases to 9.3% due to a decrease in all output parameters. Analysis of the quantitative effect of the "light" diode characteristics on the experimentally observed efficiency variation showed that the growth of η with an increase in d_{CdCl_2} to 0.6 μm equally causes a decrease in the series resistance, the diode saturation current density, and photocurrent density growth. According to the simulation data, the reduction in η to 9.3% with an increase in d_{CdCl_2} to 0.8 μm is caused by an increase in J_0 and a decrease in J_{ph}.

Comparison of the output characteristics and "light" diode parameters of the ITO/CdS/CdTe/Cu/Au and SnO_2 : F/CdS/CdTe/Cu/Au SCs shows that the high voltage and large filling factor of the structures with transparent SnO_2 : F front electrode are caused by a

Table 2. Effect of annealing in air at a temperature of 430°C for 25 min on the optical and electrical properties of the ITO and SnO_2 : F front electrodes

Front electrodes	Before annealing		After annealing	
	ITO	SnO_2 : F	ITO	SnO_2 : F
d, nm	120	380	120	380
μ, cm^2/V	27	34	30	33
n, cm^{-3}	1.8×10^{21}	3.9×10^{20}	6.0×10^{20}	3.8×10^{20}
ρ, Ω cm	1.3×10^{-4}	4.7×10^{-4}	3.5×10^{-4}	4.9×10^{-4}
$R_{\square}$, Ω/□	10.8	12.4	29.6	13.1
$T_{450-900}$, %	82.8	78.3	86.8	78.5

lower diode saturation current density and series resistance, respectively. At the same time, it should be noted that SCs with an ITO front electrode exhibit high short-circuit current density, which is caused by a higher photocurrent density.

3.2. Variations in the Crystal Structure and Properties of the Front Electrodes during the Fabrication of CdS/CdTe-Based Film SCs

In the fabrication of CdS/CdTe-based SCs, the operation with the highest temperature is "chloride" treatment, which suggests annealing in air. Therefore, we investigated the crystal structure and optical and electrical properties of the ITO and SnO_2 : F films before and after annealing in air at a temperature of 430°C for 25 min, i.e., under "chloride" treatment conditions.

It was established that, in the ITO films after "chloride" treatment of the CdS/CdTe device structure, the preferred orientation changes its direction from [001] to [111], which was estimated from the variation in the ratio between the corresponding diffraction maxima [5]. According to published data [6, 7], in the case of an oxygen deficiency, the formed ITO films are oriented in the [001] direction and in the case of an oxygen excess, in the [111] direction. This is determined by the ratio between oxygen and indium atoms in the (002) and (222) crystallographic planes, which correspond to these crystallographic directions. Therefore, the experimentally observed change in the preferred orientation direction in the investigated ITO films naturally results from high-temperature annealing in air. In addition, it was established that annealing in air broadens the diffraction maxima, i.e., causes degradation of the quality of the ITO-film crystal structure because of the occurrence of one or several negative processes: microstrain enhancement, a decrease in the coherent-scattering-region sizes, and an increase in the density of stacking faults and twins.

After annealing in air, the resistivity ρ and surface resistance $R_{\square}$ of the ITO films grew several times (Table 2). Investigation of the carrier mobility μ and majority-carrier concentration n in the ITO films before and after annealing shows that the observed resistivity reduction is caused by a decrease in n (Table 2). The reduction in the majority-carrier concentration after annealing in air can be related to a decrease in the concentration of oxygen vacancies (low-level donors) or to the transition of tin from the electrically active state (indium sublattice sites) to the electrically inert state caused by the formation of tin oxides on the developed grain boundary surface in the ITO film.

Studying the optical properties of the ITO films showed that annealing in air increases the average transmittance of the film on the glass substrate in the range 450–900 nm ($T_{450-900}$), which corresponds to the spectral range of photosensitivity of the cadmium-telluride base layers. This is apparently due to a decrease in the oxygen-vacancy concentration in the front electrode upon annealing in air.

After annealing of the SnO_2 : F films in air, no variations in the crystal structure and optical and electrical properties were observed (Table 2). This is due to the chemical inertness of fluorine and, probably, a lower oxygen-vacancy concentration in the tin-oxide films. The high stability of the SnO_2 : F crystal structure ensured a higher-quality separating barrier in the SnO_2 : F/CdS/CdTe/Cu/Au SCs, which is characterized by a lower diode saturation current density as compared with that of the ITO/CdS/CdTe/Cu/Au SCs. The lower series resistance of the SnO_2 : F/CdS/CdTe/Cu/Au SCs is caused by the lower surface resistance of the SnO_2 : F layer after annealing in air as compared with that of ITO layers (Table 2) and a larger optimal thickness of the cadmium-chloride layer upon the performance of "chloride" treatment, which allowed us to effectively dope the cadmium-telluride base layer.

Table 3. Output parameters and "light" diode characteristics of the ITO/SnO_2/CdS/CdTe/Cu/Au solar cells

Output parameters and "light" diode characteristics	d_{CdS} = 0.4 μm		d_{CdS} = 0.2 μm		
	d_{SnO_2} = 50 nm	d_{SnO_2} = 80 nm	d_{SnO_2} = 50 nm	d_{SnO_2} = 80 nm	d_{SnO_2} = 100 nm
J, mA/cm^2	20.5	19.6	21.4	20.9	20.5
U, mV	761	792	649	765	760
FF, rel. units	0.67	0.64	0.52	0.71	0.63
η, %	10.5	9.9	7.2	11.4	9.9
J_{ph}, mA/cm^2	20.8	20.3	21.6	21.3	20.7
R_n, Ω cm^2	2.2	5.4	1.8	2.8	4.2
R_{sh}, Ω cm^2	760	1200	450	800	700
A, rel. units	2.3	1.9	2.7	2.1	2.2
J_0, A/cm^2	2.7×10^{-8}	1.1×10^{-8}	4.3×10^{-7}	2.5×10^{-8}	2.8×10^{-8}

The higher photocurrent density in the ITO/CdS/CdTe/Cu/Au SCs as compared with the SnO_2 : F/CdS/CdTe/Cu/Au ones is caused by the higher transmittance of the ITO layers as compared with that of the SnO_2 : F layers (Table 2), which ensures a higher density of the photon flux entering the base layer.

3.3. Study of the ITO/SnO_2/CdS/CdTe/Cu/Au Solar Cells

To combine the high transparency of the ITO front electrodes and stability of the SnO_2 : F ones in the formation of CdS/CdTe-based SCs, we used bilayer ITO/SnO front electrodes. The cadmium-chloride thickness during chloride treatment of the ITO/SnO_2/CdS/CdTe/Cu/Au SCs was 0.6 μm, which corresponded to the optimal d_{CdCl_2} values for a SnO_2 : F/CdS/CdTe/Cu/Au SC.

Analytical processing of the "light" I–V characteristics showed that growth of the tin-oxide-layer thickness in the bilayer ITO/SnO electrodes to d_{SnO_2} = 50 nm enhances the efficiency of the ITO/SnO_2/CdS/CdTe/Cu/Au SCs to η = 10.5%. It was established that the open-circuit voltage and filling factor of the "light" I–V characteristic of the ITO/SnO_2/CdS/CdTe/Cu/Au SC are larger than in the structures with ITO front electrodes and the short-circuit current density is higher than in the SCs with the SnO_2 : F front electrode (Tables 1 and 3). The simulation shows that the growth in the efficiency of the ITO/SnO_2/CdS/CdTe/Cu/Au SCs as compared with that of the ITO/CdS/CdTe/Cu/Au SCs is caused by a decrease in the diode saturation current density and series resistance. In addition, according to the simulation data, the growth of efficiency of the ITO/SnO_2/CdS/CdTe/Cu/Au SCs as compared with that of the SnO_2 : F/CdS/CdTe/Cu/Au ones is caused by an increase in the photocurrent density.

With a further increase in the nanoscale tin-dioxide spacer layer to d_{SnO_2} = 80 nm, the open-circuit voltage increases to U = 792 mW; however, the short-circuit current density and filling factor of the "light" I–V characteristics decrease, which leads to a decrease in η to 9.9%. The simulation shows that the photocurrent-density reduction and the series-resistance enhancement play a decisive role in the efficiency drop.

According to published data [8], the significant loss in the photocurrent is caused by light absorption in the cadmium-sulphide layer. Therefore, we fabricated ITO/SnO_2/CdS/CdTe/Cu/Au SCs with a cadmium-

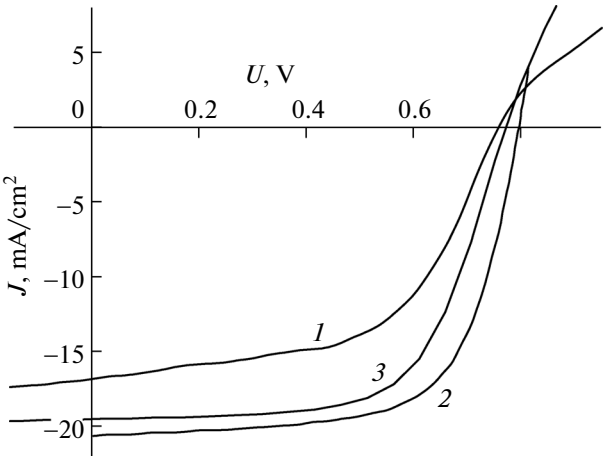

Fig. 3. "Light" I–V characteristics of the SnO_2 : F/CdS/CdTe/Cu/Au solar cells. d_{CdCl_2} = (*1*) 0.4, (*2*) 0.6, and (*3*) 0.8 μm.

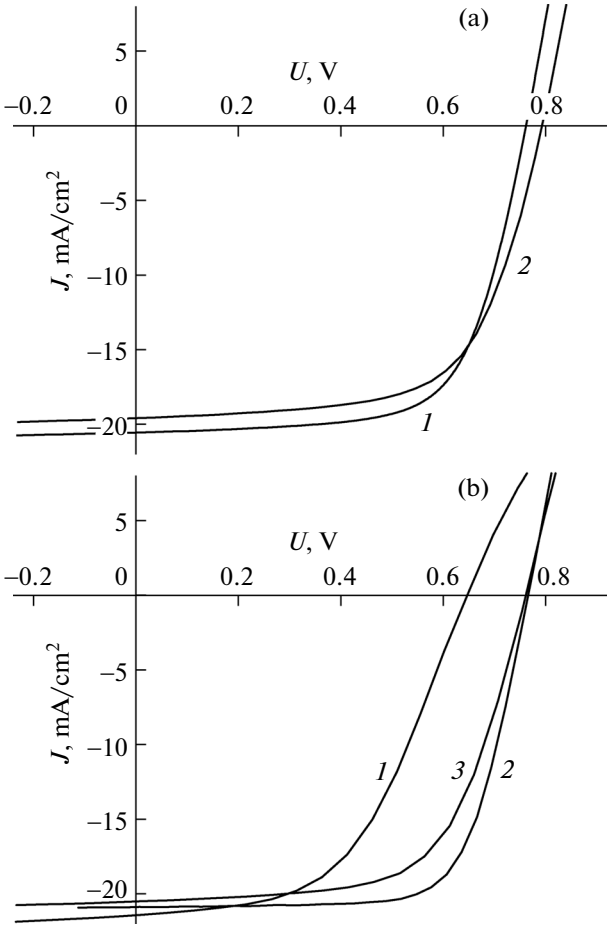

Fig. 4. "Light" I–V characteristics of the ITO/SnO_2/CdS/CdTe/Cu/Au solar cells. (a) (*1*) d_{CdS} = 0.4 μm and d_{SnO_2} = 50 nm, (*2*) d_{CdS} = 0.4 μm and d_{SnO_2} = 80 nm; (b) (*1*) d_{CdS} = 0.2 μm and d_{SnO_2} = 50 nm, (*2*) d_{CdS} = 0.2 μm and d_{SnO_2} = 80 nm, and (*3*) d_{CdS} = 0.2 μm and d_{SnO_2} = 100 nm.

sulphide-layer thickness reduced from d_{CdS} = 0.4 μm to d_{CdS} = 0.2 μm. The tin-oxide-layer thickness was d_{SnO_2} = 50 nm, which corresponded to the maximum efficiency of the ITO/SnO_2/CdS/CdTe/Cu/Au SCs at d_{CdS} = 0.4 μm. As the cadmium-sulphide-layer thickness is decreased at a tin-oxide-layer thickness of 50 nm, the short-circuit current density increases due to an increase in the density of the photon flux entering the base layer. However, in this case, the open-circuit voltage and filling factor decreased, which led to a drop of the efficiency. The simulation showed that the reduction in η is due to a decrease in the shunting resistance and an increase in the diode saturation current density. According to the results of our previous study [9], the efficiency drop with decreasing cadmium-sulphide-layer thickness is caused by shunting of the main separating barrier by the *n*-ITO–*p*-CdTe heterojunction, which, due to the significant difference in the lattice periods of the heteropartners, exhibits a high diode saturation current density and lower shunting resistance. Therefore, to exclude shunting of the main separating barrier, at a cadmium-sulphide-layer thickness of 0.2 μm, we increased the tin-oxide-layer thickness. It was established that, at a cadmium-sulphide-layer thickness of 0.2 μm, the increase in the tin-oxide-layer thickness to d_{SnO_2} = 80 nm leads to an increase in efficiency to η = 11.4%, which is attributed to an increase in the open-circuit voltage and filling factor of the "light" I–V characteristic. According to the simulation data, the observed optimization of the photoelectric processes is caused by an increase in the shunting resistance and a decrease in the diode saturation current density. Thus, the increase in the tin-oxide-layer thickness to d_{SnO_2} = 80 nm compensates a decrease in the cadmium-sulphide-layer thickness to 0.2 μm and enhances the efficiency on account of an increase in the photocurrent density and a decrease in the series resistance.

With a further increase in the tin-oxide-layer thickness to d_{SnO_2} = 100 nm, the efficiency decreases due to a decrease in the short-circuit current density and filling factor of the "light" I–V characteristic. Simulation of the effect of the diode characteristics on the SC efficiency shows that the efficiency reduction is caused by a decrease in the photocurrent density and an increase in the series resistance. It should be noted that, at a cadmium-sulphide-layer thickness of 0.2 μm, an increase in the tin-oxide-layer thickness to d_{SnO_2} = 100 nm does not lead to open-circuit voltage growth, in contrast to the observed growth of this output parameter in SCs with a cadmium-sulphide-layer thickness of 0.4 μm with an increase in the tin-oxide-layer thickness to d_{SnO_2} = 80 nm. Thus, a further reduction in the cadmium-sulphide-layer thickness can no longer be compensated by a further increase in the thickness of the tin-oxide layer.

4. CONCLUSIONS

The use of nanoscale tin-dioxide spacer layers in ITO/SnO_2/CdS/CdTe/Cu/Au SCs during "chloride treatment" of the CdS/CdTe device structures minimizes oxygen delivery to the ITO films. This makes it possible to avoid the SC efficiency limitation related to growth of the series resistance of the structure due to a decrease in the majority-carrier concentration in the ITO films. In addition, CdS/CdTe-based SCs with ITO/SnO_2 front contacts exhibit open-circuit voltage growth caused by a decrease in the diode saturation current density due to stabilization of the ITO-film crystal structure against "chloride treatment."

The nanoscale high-resistance tin-dioxide spacer layer at the ITO/CdS interface allows shunting of the main separating barrier by the *n*-ITO–*p*-CdTe heterojunction with decreasing CdS-layer thickness to be prevented to enhance the density of the photon flux entering the CdTe base layer. As the cadmium-sulphide-layer thickness is decreased to 0.2 μm, at a tin-oxide layer of 80 nm the efficiency of the ITO/SnO_2/CdS/CdTe/Cu/Au SC laboratory samples attain 11.4%.

REFERENCES

1. J. Han, C. Spanheimer, G. Haindl, et al., Solar Energy Mater. Solar Cells **95**, 816 (2011).
2. M. Hadrich, C. Heisler, U. Reislohner, C. Kraft, and H. Metzner, Thin Solid Films **519**, 7156 (2011).
3. M. A. Martinez, C. Gullien, C. Gutierrez, and J. Herrero, Solar Energy Mater. Solar Cells **43**, 297 (1996).
4. H. S. Raushenbach, *Solar Cells Array Design* (Litton Education Publishing, New York, 1980).
5. H. R. Moutinho, F. S. Hasoon, F. Abulfotuh, and K. Kazmerski, J. Vacuum Sci. Technol. A **13**, 2877 (1995).
6. G. Guillen and J. Herrero, Vacuum **67**, 611 (2002).
7. G. Guillen and J. Herrero, Thin Solid Films **431–432**, 403 (2003).
8. L. A. Kosyachenko, E. V. Grushko, and X. Mathew, Solar Energy Mater. Solar Cells **96**, 231 (2012).
9. G. S. Khripunov, B. T. Boiko, G. I. Kopach, et al., Nauch. Vestn. Chernovetsk. Univ. **237**, 80 (2005).

Translated by E. Bondareva